RECENT ADVANCES IN COMPOSITES BY CHARACTERIZATION OF GRAPHEME OXIDE FOR HIGH PERFORMANCE APPLICATIONS

Ms.Rajni Devi[1], Dr.Anupam selot[2],
[1] *Ph.d Scholar, Physics , SSSUTMS Sehore, Madhya Pradesh, India*
[2] *Professor, Physics , SSSUTMS Sehore, Madhya Pradesh, India*

ABSTRACT

Growing concerns about energy and environmental problems over the past decades have allowed researchers to focus more on water treatment with a spread of techniques and to form portable water suitable for renewable purposes. Likewise the present energy problem are often solved by building hybrid electrode materials with improved performance that not only solves the issues but also helps us to beat future energy demand. Graphene has received a good range of attention in its use in nano electronics, catalysis, batteries, sensors and super capacitors. thanks to the superb and distinct properties of graphene like the vast earth, high electron mobility and energy efficiency, high thermal stability and mechanical properties, the essence is as powerful as electro catalyst and provides advances within the field of electrochemistry. The union of GO and metal oxide nano composites removes barriers to their individual operation. during this article the thesis graphene oxide was used because the basic matrix for the formation of metal oxides, plasmonic and ternary composites and was observed, tested for exposure to sunlight driven by photo catalysis and enormous electrodes.

Keyword : - *Nano electronics, Super capacitors, Composite Materials, Photo catalysis, Electrodes.*

1. INTRODUCTION

The word carbon is derived from the Latin word 'carbo' which means coal that makes allotropes stable. Carbon with sp3 hybridization creates a diamond with a tetrahedral lattice, sp2 hybridization leads to the formation of graphite. The last 30 years have led to the discovery of many other carbon allotropes such as buckminsterfullerene (C60), carbon nanotubes (CNTs) and graphene (Lee et al 2008) as shown in Figure 1.1. Carbon steel has attracted much interest in its various uses due to its durability, performance, stability, and relative environmental friendliness. Various carbon materials such as activated carbon (AC), carbon porous, low-cost carbon and high-quality carbon airgel are widely used in the advertising process (Goel et al 2005) and as electrode materials in super capacitors (Inagaki et al 2010) . Chemical stability at high temperatures in acidic or basic solution makes carbon an attractive material to be used as electrodes for electrochemical energy devices (Hou et al 2011). Carbon serves as a source for the integration of various graphitic elements. However, a change in the history of carbon came about through the discovery of graphene, which has unusual properties.

Graphene

Graphene is the name given to a single layer of carbon atoms (sp2) with a bond length of 0.142 nm, in a closely arranged honeycomb two-dimensional (2D) network. It consists of two equivalent sub-lattices of carbon atoms bonded with σ bond, which is a basic building block for all other graphitic materials of various dimensionalities (Geim & Novoselov 2007, Peres 2009). The fundamental insight into all other forms of carbon materials can be outlined by studying graphene (Segal 2009). Other forms of carbon allotropes that are derived from graphene are graphite (3D (three-dimension)) which can be considered as a stack of graphene (2D) layers, carbon nanotubes (1D (one-dimension)), which are rolled sheets of graphene, and buckminsterfullerene (0D, C60), which consists of graphene balled into a sphere through incorporation of some pentagons and hexagons into the lattice. Carbon nanotubes (CNTs) are very similar to graphene materials; if a single-walled carbon nanotubes (SWCNTs), were to be cut down at one edge and flattened out, it's called a graphene sheet or carbon nanosheet. On the contrary, if a sheet of graphene were to be rolled up into the shape of a straw, it would then be called carbon nanotubes. Graphene is simply a single layer of graphite. A single sheet of graphite, however, has properties significantly different from multi-layer graphite.

Properties of graphene (Wu 2012)

S.No.	Properties of grapheme	Values
1.	Theoretical specific area	2620 m^2g^{-1}
2.	Intrinsic mobility	200 000 cm^2 $v^{-1}s^{-1}$
3.	Young's modulus	1.0 TPa
4.	Fracture strength (stiffness)	130 GPa
5.	Thermal conductivity (100 times that of Cu)	5000 $Wm^{-1}K^{-1}$
6.	Optical transmittance (absorbs 2.3% of white light)	97.7%
7.	Electrical conductivity (single layer graphene)	649 S cm^{-1}
8.	Breaking strength	42 Nm^{-1}
9.	Electron mobility (lower than Ag)	15000 cm^2 V^{-1} cm^{-1}
10.	Electrochemical potential window	2.5 V in 0.1M PBS, pH 7
11.	Fermi velocity (similar to speed of light)	10^6 m s^{-1}

Graphene Oxide

Although graphene can be obtained by the above mentioned methods, they are constrained by low yield, high cost and/or processing limitations. Current approaches of preparing graphene involve the initial oxidation of graphite to graphite oxide, followed by the mechanochemical or thermal exfoliation of graphitic oxide to graphene oxide (GO) sheets. Their eventual reduction to graphene has attracted much attention because of the facile scalability and high yield. GO is the hydrophilic derivative of graphene with thickness around 1nm and lateral dimension varying between few nanometers and several microns. Graphite oxide is heavily oxidized form of graphene that consists of single layer of graphene sheets bearing carboxyl, epoxide and hydroxyl functional groups on their basal plane linked to C-sp3 structure (Dreyer et al 2010). Based on the chemical analysis the carbon to oxygen ratio in GO was approximately found to be 3:1 (Stankovich et al 2006). The functional groups present in the basal and peripheral region give rise to various properties in GO. The carboxyl and carboxylic acid moieties present at the edges (-COOH) are responsible for the negative surface charge which is pH dependent and affords colloidal stability to the GO suspension (Park et al 2009b). The basal plane containing the epoxide (-O-) and alcohol (hydroxyl (-OH)) groups are responsible for the surface reactions and hydrogen bonding.

2. LITERATURE REVIEW

(Yin et al 2013), thermal reduction (Zhu et al 2011), microwave assisted reduction (Hassan et al 2009), electrochemical reduction (Ramesh & Sampath 2009) and photochemical reduction (Matsumoto et al 2010) etc. Among the various methods of reduction chemical reduction is considered to be the most versatile route involving a wide array of reducing agent owing to its ability to produce graphene/rGO in large scale compared to other synthesis route

(Qi et al 2010b),Wastewater from textile and food industries mainly constitutes dyes used for dyeing and as food colouring agents. Dyes are used in various other applications like biological staining, tracers, coloration of paper, ELISA (enzyme linked immune assay), etc. These are toxic organic pollutants that affect the environment and aquatic life. When humans consume these dye contaminated water they also get affected as most of these dyes are found tobe carcinogenic (Hui et al 2011). To prevent disruption of the ecosystem and protect our environment, it is imperative to treat the dye contaminated wastewater before they are released into water bodies. But their structural complexity makes their treatment a herculean task.

Over the years, many technologies have been developed for the treatment of dye contaminated waters. Adsorption is one of the most commonly used methods for mineralization of dye due to low cost and simplicity. But, the major drawback of this process lies in the fact that the dye is not degraded but simply adsorbed onto a solid adsorbent surface, which needs further treatment. Also during regeneration of the adsorbent, the dye is released into another medium, which again needs further treatment (Jenny et al 2014).

Electrochemical processes like electrooxidation are highly efficient in completely degrading the dye; nevertheless, it suffers from the disadvantage of high cost and high energy consumption. With the whole world suffering from energy crisis, it would not be prudent to use such a technology for treating high volumes of wastewater (Lam et al 2012). Biological processes on the other hand help in cutting down the costs and energy consumption, but it takes longer time for completion. Also, the residual sludge needs to be disposed after another round of treatment process. Hence, it is vital to develop new technologies that can minimize these drawbacks for the optimal treatment of these harmful organic pollutants.

Photocatalysis is the process in which light activated catalyst drives the reaction to degrade the organic pollutants. The acceleration of the reaction occurs due to the ability of the catalyst to generate electron-hole pairs leading to the generation of free radicals which stimulates secondary reactions. Metal oxide nanoparticles are used in many applications such as catalysis, sensing, etc with both biological and environmental importance (Chen 2007). Their large surface area and higher chemical reactivity have procured them an inimitable position in various strata of technology. Environmental pollutant degradation is one such area where metal oxide nanoparticles have cemented its position.

A variety of semiconductor photocatalysts have been used for the synthesis of graphene based composites. Metal oxides such as TiO2, ZnO, SnO2, Fe2O3, Cu2O and slats such as ZnS, CdS, BiVO4, Bi2WO6, ZnFe2O4, metal free polymer and silver/silver halides such as Ag/AgCl and Ag/AgBr etc are most widely considered under semiconductor photocatalysis. Semiconductor based photocatalysis using TiO2 has been used for many decades for degradation of organic pollutants. Among the various candidates for photocatalysts TiO2 is the only material till date for industrial applications and considered as the benchmark in the area of photocatalysts. It has been extensively studied due to its good stability, high photoreactivity, high efficiency, low cost, less toxicity and

environmental friendly nature (Chen & Mao 2007). The crucial breakthrough in research on TiO2 photocatalysis paved way for many practical applications as stated by Jenny and his co-workers in their review article

(Jenny et al 2014). In 1972 Honda and Fujishima discovered the electrolysis of H2O using TiO2 photoanode with UV irradiation (Fujishima & Honda 1972). One of the major drawbacks of using TiO2 is the use of UV irradiation for its activation. In order to improve its visible light activity, various modification methods such as dye sensitization semiconductor coupling, doping etc have been performed in recent years. After these modifications TiO2 showed visible light absorption with boosted photocatalytic efficiency (Jenny et al 2014).

John et al (2011) evaluated the degradation of Rhodamine B (RhB) dye under visible light using ZnO nanocrystalline materials with different particle and crystal sizes. Three different solvents such as ethanol, methanol and propanol were used to synthesis ZnO by solvothermal method. It was observed that the ZnO synthesized using methanol as solvent has a smaller crystallite size of 4.8 nm and average particle diameter of 19.8 nm. The smaller particle sized ZnO shows an improved photocatalytic application than ZnO obtained by other solvents. Based on this it was concluded that the crystallinity plays a crucial role in improving the photocatalytic performance.

Jian et al (2009) reported a novel dumbbell-shaped ZnO microcrystal photocatalyst and evaluated its performance for the degradation of three different kinds of dye contaminated wastewater. The degradation efficiency of methyl violet (MV) and methylene blue (MB) dye wastewater using the synthesized dumbbell shaped ZnO nanoparticles was found to be 99 % and 98.5 % respectively. The TOC removal efficiency of the obtained ZnO nanoparticle was nearly 16-22 % higher than the commercial ZnO. A ZnO nanowire array synthesized by microwave assited hydrothermal method was reported recently by Xing et al (2015). The experimental results suggest that the ZnO nanowires have high photocatalytic activity towards the degradation of methyl orange (MO) dye containing wastewater in 75 min of exposure.

Han et al (2012) reported hierarchical ZnO flower-rod arrays (FRs) on indium doped tin oxide (ITO) glass using ZnO as a seed layer. The CV studies revealed that the ZnO FRs exhibit a higher current density than ZnO nanoparticles in the oxidative decomposition of RhB. The photo-electrochemical properties and the mechanism of the photodegradation is validated with C-V curves and I-t curves. The degradation efficiency of RhB using ZnO FRs was nearly 100% with an irradiation time of 1.5 h.

Apart from the most widely used TiO2, ZnO photocatalysts various other metal oxide photocatalysts have also been reported. SnO2 nanocrystals (Wu et al 2009) was synthesized by hydrothermal synthesis with the aid of amino acid and used for the degradation of RhB. Boxiang et al (2012) synthesized SnO2 microflowers. In 1998, Hara and his co-workers in 1998 reported the water splitting under visible light using Cu2O photocatalyst. The most crucial aspect of Cu2O photocatalyst is the excess evolution of O2 on the surface/bulk leading to p-type semiconducting nature. Cu2O with varying morphologies have been synthesized by means of reduction route with surfactants. It was confirmed that the Cu2O polyhedrons exhibits higher photocatalytic activity than the Cu2O nanoparticles (Poonam & Shatendra 2012). Semiconductors like Fe2O3 (Troy et al 2011), WO3 (Wang et al 2014b, An et al 2012b), CdS

(Qin et al 2013), ZnS (Dagui et al 2010) etc are also found to be a suitable materials for photocatalysis. Various TMOs have been employed as photocatalytic materials and extensively studied over the past years. TMOs with different morphologies such as micro/nanoparticles, nanotubes, nanowires, nanoflowers, and other hierarchical morphologies have also attracted the researchers (Chen & Caruso 2013). These specialized morphologies assist in enhancing the charge transfer and thereby reducing the charge recombination. In order to further enhance the performance of TMOs based photocatalytic materials, composites based on carbonaceous materials such as graphene (Liang et al 2010), activated carbon, CNTs (An et al 2007) etc have been explored. Graphene is of particular interest owing to its conjugated planar surface and high electron mobility which improves the charge transfer properties (Fan et al 2011).

3. MATERIALS AND METHODS

Methylene blue dye was selected as the model dye for the photocatalytic treatment using the synthesized Ag/AgCl/GO and ZnO/GO nanocomposites. MB dye is of low molecular weight and the photocatalytic performance of the various photocatalyst were analysed with MB dye. Based on its performance the photocatalyst can be employed for other types of dyes. The UV-Vis spectrophotometer was used for the decolourization studies at λmax of 668 nm and the degradation of MB was investigated. The physical characteristics and the molecular structure of MB dye are tabulated in Table 3.1. For photocatalytic reaction, 5 mL (10 mg mL-1) of dispersed suspension of the as-synthesized nanostructures was transferred to a 250 mL beaker containing 45 mL aqueous solution of MB (10 mg L-1). The dispersion was kept in the dark for 30 min so that the dye molecules and catalysts achieve equilibrium after which the decolourization was accomplished in sunlight i.e solar light irradiation. The UV light flux was 5400 Lux (4% from 135000 of visible light) as measured using LUX Meter (LX-101), LT Lutron, Taiwan. 2 mL of dye solution was taken at regular intervals, centrifuged and the absorbance was recorded using UV spectrophotometer (Shimadzu 1800) at 668 nm.

Physical characteristics of methylene blue dye

Dye name	**Methylene blue**
Abbreviation	MB
C.I. name	Basic Blue 9
C.I. number	52015
Class	Thiazin
$^{\lambda}$max	668 nm
Colour	Blue
Empirical formula	$C_{16}H_{18}N_3SCl$
Formula weight	319.9 g mol^{-1}
Molecular volume	241.9 cm^3 mol^{-1}
Molecular diameter	0.80 nm
Molecular weight	356 g mol^{-1}
ε	79.15 x 10^3 (L mol^{-1} cm^{-1})
Molecular structure	

Electrochemical Supercapacitors

Ferrous sulphate heptahydrate (FeSO4.7H2O), polyvinylpyrrolidone (PVP), hydrochloric acid (HCl), DD water were purchased from SRL chemicals. Iron ore tailings, collected from local iron ore industries and the samples were analysed for higher content of iron by ICP-OES analysis and the sample with high iron content of 45.2% was used in the present study. All other chemicals were of analytical reagent grade. A weighed amount of IOTs was acid leached with HCl (1:1) at 900C in order to leach out the iron content. The acid insoluble portion was separated by filtration and the filtrate containing FeCl3 was treated with calculated amount of hydrogen peroxide (H2O2). Filtrate was heated to 60°C, and its pH was maintained below 4 by adding an appropriate amount of concentrated ammonia. As a result, iron was separated from tailings and precipitated into Fe(OH)3. Finally, Fe(OH)3 was washed repeatedly with de-ionized water, Then FeCl3 solution was obtained by Fe(OH)3 precipitate dissolution with hydrochloric acid (1:1) (Shen et al 2012). GO was synthesized by the previously reported procedure (Yang et al 2012b). To the ferric chloride solution obtained from IOTs where the % weight of Fe is (36.45%), calculated amount of FeSO4.7H2O

(2:1), 0.60 g PVP and 30 mL as-prepared GO solution (3 mg mL-1) were added and the solution was mixed with 30 mL deionized water and magnetically stirred for 30 min at 500 rpm.

Aqueous ammonia solution (5mL) was added in drops to the above solution and again stirred for 30 min at 500 rpm to ensure complete ion exchange. The solution was transferred to 90 mL teflon-lined stainless steel autoclave and maintained at 1600C for 12 h. The resulting solution was cooled at room temperature and the black solid mass was collected by filtration, washed with ethanol and DI water each for several times and dried at 800C in vacuum oven. Bare Fe3O4 was also synthesized for comparison from IOTs. A weighed amount of IOTs was acid leached with HCl (1:1) at 900C in order to leach out the iron content. The filtrate containing FeCl3 was separated by filtration and the filtrate was treated with hydrogen peroxide (H2O2). The filtrate was heated to 60°C, at pH below 4 by using concentrated ammonia. As a result, iron was separated from tailings and precipitated into Fe(OH)3, washed repeatedly with de-ionized water. From which FeCl3 solution is obtained by using HCl (1:1). To the ferric chloride solution obtained from calculated amount of FeSO4.7H2O (2:1), 0.60 g PVP was added and the solution was mixed with 30 mL deionized water and stirred at 500 rpm for 30 min. After the addition of ammonia the entire mixture was again stirred at the same rpm for 30 min and autoclaved for 12h at 160°C. The product was cooled and washed repeatedly with DD water and dried.

4. RESULTS AND DISCUSSION

Characterization

The FTIR spectra of the synthesized GO and ZnO/GO nanocomposite are shown in Figure 4.1(a). The peak at 1720 cm-1 corresponds to the C=O stretching, 1627 cm-1 arises from C=C stretching vibration, stretching at 1404 cm-1, 1226 cm-1 and 1057 cm-1 is due to C-OH and CO stretching vibrations from the epoxy and alkoxy group respectively (Marcano et al 2010). The spectra of ZnO/GO nanocomposite show peaks at 1562 cm-1 and small peak at 1420 cm-1 corresponding to the antisymmetrical and symmetrical vibrations of the zinc carboxylate respectively. The band at nearly 3500 cm-1 is assigned to the –OH stretching frequency of hydroxyl group (Xu et al 2008) affirming the formation of ZnO nanoparticles decorated on the GO matrix.

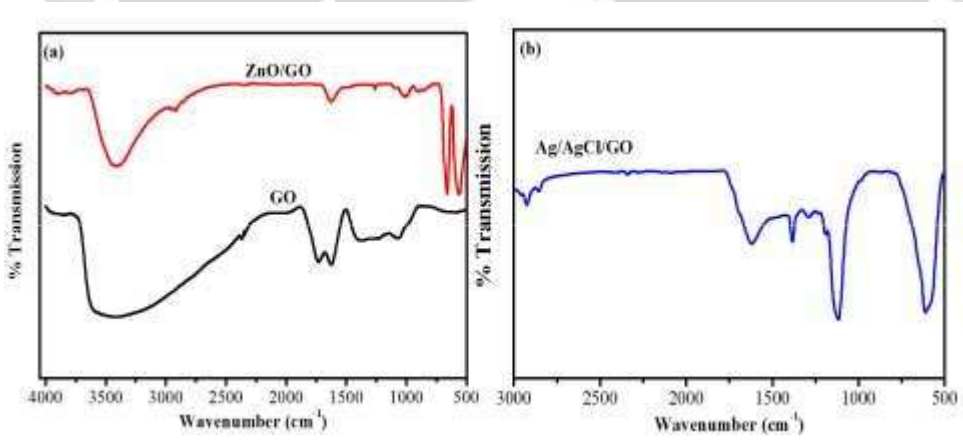

FTIR Spectra of (a) GO, ZnO/GO and (b) Ag/AgCl/GO nanocomposite

4.2XRD studies

XRD studies was used to examine the structural changes originating from the oxidation of graphite to graphene oxide (GO) and also
the formation of Ag/AgCl/GO and ZnO/GO nanocomposite obtained by low temperature hydrothermal synthesis. Figure 4.2 shows the XRD pattern of Ag/AgCl/GO nanocomposite and GO. GO exhibits an intense and sharp peak at 10.460 assigned to (001) plane (Nethravathi et al 2008). The enhanced interplanar distance of GO when compared to the pristine graphite which displays its characteristic peak at nearly 260 with (002) plane (Jeong et al 2008) is because of the intercalated oxygen containing

functional groups in GO. The XRD pattern of Ag/AgCl/GO photocatalyst synthesized using mild reducing agent and was investigated to examine the formation of Ag/AgCl/GO nanocomposite.

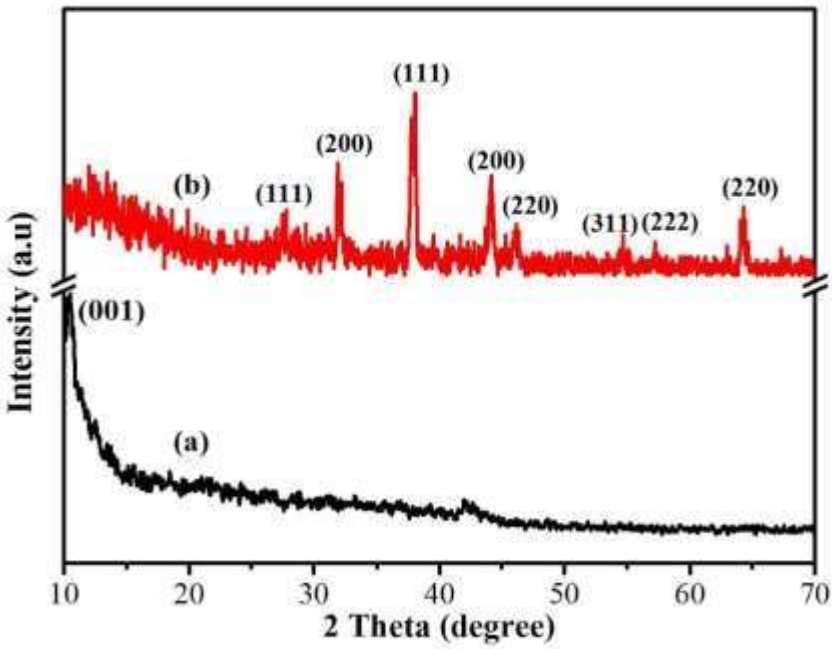

XRD of (a) GO and (b) Ag/AgCl/GO nanocomposite

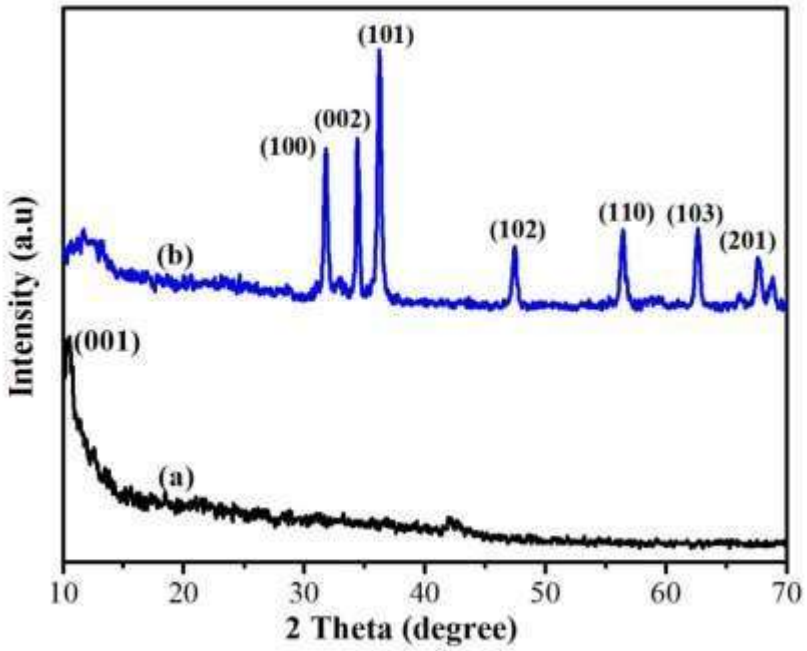

XRD of (a) GO and (b) ZnO/GO nanocomposite

5. CONCLUSIONS

This dissertation investigates the applications of graphene based composites in the photocatalysis and supercapacitor applications. The graphene which serves as the matrix for the growth of metal oxide/metal halides and metal nanoparticles was prepared by Hummers method. It is further modified with metal oxides, metal halides and noble metals and used for various applications.

For photocatalytic degradation of MB dye, ZnO/GO and Ag/AgCl/GO nanocomposite were developed by a low temperature hydrothermal method. The resulting photocatalysts was characterized by various instrumental methods to study their structure, size, morphology, elemental composition, chemical composition and surface properties. The XRD and EDAX analysis confirms the formation of GO and successful incorporation of ZnO and Ag/AgCl on GO matrix. Clubbing of GO with ZnO, ie., ZnO/GO nanocomposite have shown good photocatalytic performance owing to the reduction of the recombination of charge carriers on the catalysts surface leading to structural changes, required for an efficient photocatalyst. The Ag/AgCl/GO nanocomposite effectively absorbs the incident photons due to the confined SPR excitation of Ag nanoparticles existing in the visible region, reinforcing the separation of photogenerated electron and hole pair. The visible light absorption of Ag/AgCl is due to the presence of plasmonic absorption of Ag nanocrystals, since AgCl alone can't absorb visible light due to the wide band gap of 3.32 eV leading to difficulty in excitation in visible light and also it is found to be unstable under sunlight. The presence of Ag nanoparticles on AgCl enhances the absorption of visible light due to the strong SPR effect.

6. REFERENCES

1. Ahmed, KAM, Zeng, QM, Wu, KB & Huang, KX 2010, Mn3O4 nanoplates and nanoparticles: Synthesis, characterization, electrochemical and catalytic properties', Journal of Solid State Chemistry, vol. 183, no.3, pp. 744-751.

2. Akpan, UG & Hameed, BH 2009, 'Parameters affecting the photocatalytic degradation of dyes using TiO2-based photocatalysts: A review', Journal of Hazardous Materials, vol. 170, no. 2, pp. 520-529.

3. Aleksandra BD, Leunga, YH & Alan, MCN 2014, 'Strategies for improving the efficiency of semiconductor metal oxide photo catalysis, Material Horizons, vol. 1, no. 4, pp. 400-410.

4. Amrita, J & Tripathi, SK 2013, 'Converting eucalyptus leaves into mesoporous carbon for its application in quasi solid state supercapacitors', Journal of Solid State Electrochemistry, vol. 17, no. 9, pp. 2545-2550.

5. An, C, Ming, X, Wang, J & Wang, S 2012, 'Construction of magnetic visible-light-driven plasmonic Fe3O4@SiO2@AgCl:Ag nano photo catalyst', Journal of Material Chemistry, vol. 22, no. 11, pp. 5171-5176.

6. An, C, Peng, S & Sun, Y 2010, 'Facile synthesis of sunlight driven AgCl:Ag plasmonic nanophotocatalyst', Advanced Materials, vol. 22, no. 23, pp. 2570-2574.

7. An, G, Ma, W, Sun, Z, Liu, Z, Han, B, Miao, S, Miao, Z & Ding, K 2007, 'Preparation of titania/carbon nanotubes composites using supercritical ethanol and their photocatalytic activity for phenol degradation under visible light irradiation', Carbon, vol. 45, no. 11,pp. 1795-1801.

8. An, X, Yu, JC, Wang, Y, Hu, Y, Yu, X & Zhang, G 2012, 'WO3 nanorods/graphene nanocomposites for high efficiency visible light driven photocatalysis and NO2 gas sensing', vol. 22, no. 17, pp. 8525-8531.

9. Arava, LMR, Manikoth, MS, Sanketh, RG & Pulickel, MA 2010, 'Multisegmented Au-MnO2/carbon nanotubes hybrid coaxial arrays for high-power supercapacitor applications', Journal of Physical Chemistry C, vol. 114, no. 1, pp. 658-663.

10. Babakhani, B & Ivey, DG 2010, 'Anodic deposition of manganese oxide electrodes with rod-like structure for application as electrochemical capacitors', Journal of Power Sources, vol. 195, no. 7, pp. 2110-2117.

11. Bell, NJ, Ng, YH, Du, AJ, Coster, H, Smith, SC & Amal, R 2011, 'Understanding the enhancement in photo electrochemical properties of photo catalytically prepared TiO2-reduced graphene oxide composite', Journal of Physical Chemistry C, vol. 115, no. 13, pp. 6004-6009.

12. Benxia, L, Tongxuah, L, Yanfen, W & Zhoufeng, W 2012, 'ZnO/graphene-oxide nanocomposite with remarkably enhanced visible-light-driven photocatalytic performance', Journal of Colloid and Interface Science, vol. 377, no. 1, pp. 114-121.

13. Berger, C, Song, Z, Li, T, Li, X, Ogbazghi, AY, Feng, R, Dai, Z, Alexei, N, Conrad, ME, First, PN & De Heer, WA 2004, Ultrathin epitaxial graphite: 2D electron gas properties and a route toward graphene-based nanoelectronics', Journal of Physical Chemistry B, vol. 108, no. 52, pp. 19912-19916.

14. Bohlen, OKJ & Sauer DU 2007, 'Ageing behaviour of electrochemical double layer capacitors: part I. Experimental study and ageing model', Journal of Power Sources, vol. 172, no. 1, pp. 468-475.

15. Boos, DL 1970, Electrolytic capacitor having carbon paste electrodes, US Patent 3536963.

16. Boxiang, J, Weina, J, Xiang, W & Fengyu, Q 2012, 'Hierarchical porous SnO2 microflowers photocatalyst', Science of Advanced Materials, vol. 4, no. 11, pp. 1127-1133.

17. Brodie, BC 1859, 'On the atomic weight of graphite', Philosophical transactions of the Royal Society of London, vol. 149, pp. 249-259.

18. Cao, CY, Qu, J, Yan, WS, Zhu, JF, Wu, ZY & Song, WG 2012, 'Low-cost synthesis of flowerlike α-Fe2O3 nanostructures for heavy metal ion removal: adsorption property and mechanism', Langmuir, vol. 28, no. 9, pp. 4573-4579.

19. Chen, DH & Caruso, RA 2013, 'Recent progress in the synthesis of spherical titania nanostructures and their applications', Advanced Functional Materials, vol. 23, no. 11, pp. 1356-1374.

20. Chen, LY, Zhang, WD, Xu, B & Xiang, YY 2012, 'A facile hydrothermal strategy for synthesis of SnO2 nanorods-graphene nanocomposites', Journal of Nanoscience and Nanotechnology, vol. 12, no. 9, pp. 6921-6929.